Original Article

Prediction of type 2 diabetes mellitus using noninvasive MRI quantitation of visceral abdominal adiposity tissue volume

Meng Wang[1#], Yanji Luo[1#], Huasong Cai[1], Ling Xu[2], Mengqi Huang[1], Chang Li[1], Zhi Dong[1], Zi-Ping Li[1], Shi-Ting Feng[1]

[1]Department of Radiology, the First Affiliated Hospital, Sun Yat-Sen University, Guangzhou 510080, China; [2]Faculty of Medicine and Dentistry, University of Western Australia, Perth, Australia

[#]These authors contributed equally to this work.

Correspondence to: Zi-Ping Li, PhD; Shi-Ting Feng, PhD. Department of Radiology, the First Affiliated Hospital, Sun Yat-Sen University, 58 Zhongshan Second Road, Guangzhou 510080, China. Email: liziping163@163.com; fengsht@mail.sysu.edu.cn.

Background: The correlation between visceral adipose tissue volume (VATV), hepatic proton-density fat fraction (PDFF), and pancreatic PDFF has been previously studied to predict the presence of type 2 diabetes mellitus (T2DM). This study investigated VATV quantitation in patients with T2DM, prediabetes, and normal glucose tolerance (NGT) using MRI to assess the roles of VATV, hepatic, and pancreatic PDFF in predicting the presence of T2DM.

Methods: Forty-eight patients with a new clinical diagnosis of T2DM (n=15), prediabetes (n=17), or NGT (n=16) were included and underwent abdominal magnetic resonance imaging (MRI) scanning with the iterative decomposition of water and fat with echo asymmetry and least square estimation image quantification (IDEAL-IQ) sequencing. VATV was obtained at the level of the 2nd and 3rd lumbar vertebral bodies (VATV L2 and VATV L3) where the sum of VATV L2 and VATV L3 (total VATV) were computed, respectively. Also, pancreatic and hepatic fat content was quantified by measuring the PDFF. The receiver operating characteristic (ROC) curve and binary logistics regression model analysis were employed to evaluate their ability to predict the presence of T2DM.

Results: The VATV L2, VATV L3, and total VATV values of the T2DM group were significantly higher than the prediabetes and NGT groups ($P<0.05$). There was no statistically significant difference between the values of VATV L2, VATV L3, and total VATV between the prediabetes and NGT groups ($P>0.05$). The ROC curve showed the areas under the curve for VATV L2, VATV L3, total VATV, hepatic PDFF, and pancreatic PDFF were 0.76, 0.80, 0.80, 0.79, and 0.75, respectively, in predicting the presence of T2DM ($P<0.01$). The ROC curves of VATV L2, VATV L3, total VATV, hepatic PDFF, and pancreatic PDFF failed to predict the presence of prediabetes and NGT ($P>0.05$). The binary logistics regression model analysis revealed that only VATV L3 was independently associated with the incidence of T2DM ($P=0.01$ and OR =1.01). The sensitivity, specificity, and total accuracy were 80.00%, 88.20%, and 84.40%, respectively.

Conclusions: Compared with hepatic PDFF, pancreatic PDFF, VAVT L2, and total VATV, VAVT L3 was the better predictor of T2DM.

Keywords: Type 2 diabetes mellitus (T2DM); visceral adipose tissue volume (VATV); quantitation; magnetic resonance imaging (MRI)

Submitted Dec 03, 2018. Accepted for publication May 30, 2019.
doi: 10.21037/qims.2019.06.01
View this article at: http://dx.doi.org/10.21037/qims.2019.06.01

Introduction

The incidence of type 2 diabetes mellitus (T2DM) has significantly increased in the past decades, resulting in higher rates of hospitalization and cardiovascular morbidity and mortality (1-3). Impaired fasting glucose (IFG) and impaired glucose tolerance (IGT) identify a group of patients at risk of developing T2DM, where abnormalities in glucose metabolism are present, but the elevation in glucose does not meet the diagnosis of T2DM (4). Currently, emerging evidence has suggested that visceral adipose tissue (VAT) represents a much higher risk for T2DM (5,6). Previous studies such as those conducted by Neeland (7) and Wander (8) reported that VAT was independently associated with a higher incidence of prediabetes and T2DM in adults. However, the available data suggest that increased hepatic and pancreatic fat content is more commonly observed in prediabetic and diabetic patients (9-11). However, some studies have reported inconsistent results when exploring the direct association between T2DM and pancreatic fat content (12-14). One explanation for this inconsistency may be the various imaging modalities used for pancreatic fat content assessment (15,16). To the best of our knowledge, few reports have compared the association of T2DM and ectopic adipose deposition (such as the VAT, liver, and pancreas fat content), and ectopic adipose deposition as a predictor of T2DM has not been previously evaluated at all.

Magnetic resonance imaging (MRI) and computed tomography (CT) are well-established gold-standard methods to assess whole-body VAT. Given its nonionizing and high nature soft tissue contrast, MRI may be particularly suited and is used by most investigators (17). The MRI protocol for iterative decomposition of water and fat with echo asymmetry and least square estimation image quantification (IDEAL-IQ) sequence is a new method with 6 echo times where fat and water can be separated (17,18). With a low flip angle to suppress the T1 effects and multiecho acquisition permit correction of the T2 effects, the IDEAL-IQ sequence leads to a more accurate modeling of the measurement of triglyceride fat content. Idilman *et al.* recently reported that IDEAL-IQ could accurately quantify hepatic fat deposition with good correlations observed between hepatic magnetic resonance spectroscopy and liver biopsy (18-20). The IDEAL-IQ sequence was also used to measure the VAT and the pancreatic fat content in a single acquisition (17,21). However, the manual assessment of whole-body VAT is time-consuming and costly, and for this reason, several previous studies already used the regional visceral adipose tissue volume (VATV) to approximate and estimate the whole-body VATV. Some studies revealed that images in the higher abdomen (around the L2–L3 region) have significantly greater predictive values of total VAT volume (22). Furthermore, other studies reported VAT at the level of the 3rd lumbar vertebra had the highest correlation to the total VATV (23,24).

The objective of this study was to use a data set of IDEAL-IQ MRI from prediabetes, T2DM, and nondiabetic adults. The aim was to measure VATV at the level of the 2nd lumbar vertebrae (VATV L2), 3rd lumbar vertebrae level (VATV L3), total VATV (VATV L2 and VATV L3), and hepatic and pancreatic proton-density fat fraction (PDFF) to investigate the differences in VATV in cohorts of patients with prediabetes, T2DM, and normal glucose tolerance (NGT). Specifically, VATV L2, VATV L3, total VATV, and hepatic and pancreatic PDFF were compared for their ability to predict the presence or absence of T2DM.

For those with undiagnosed asymptomatic prediabetes or T2DM, routine serum glucose levels may not have been tested to prompt the diagnosis and appropriate treatment. Most patients with suspected metabolic syndrome often present with incidental fatty livers where abdominal MR imaging is routinely performed to monitor the liver fat content. Our study can predict the risk of diabetes mellitus by measuring ectopic fat deposition. This can prompt further testing appropriate for clinical diagnosis where treatment can be commenced. Furthermore, for patients who have been diagnosed with T2DM, MR fat quantitative measurement can also be used to monitor the progression of diabetes mellitus, allowing for a more comprehensive assessment when combined with biochemical tests.

Methods

Patients

The study protocol was approved by the Institutional Review Board of the First Affiliated Hospital of Sun Yat-Sen University and all of the patients enrolled provided written informed consent for participation. All of the study methods were carried out in accordance with the approved guidelines.

A total of 48 subjects were enrolled in the study (18 men, 30 women; aged 51.5±8.6, 26–68 years) from November 2015 to March 2017, including patients and healthy volunteers at our institution. Diagnoses of prediabetes, T2DM, and NGT were made by the 2013 criteria of the American Diabetes Association (25) as listed in *Table 1*.

Table 1 Criteria for the diagnosis of T2DM, prediabetes, and NGT

Classification	Criteria
T2DM	T2MD was defined as a fasting plasma glucose (FPG) ≥7.0 mmol/L or 2-h plasma glucose ≥11.1 mmol/L following 75-g oral glucose load or in a patient with classic symptoms of hyperglycemia or hyperglycemic crisis, a random plasma glucose ≥200 mg/dL (11.1 mmol/L) or HbA1C ≥6.5% (the test should be performed in a laboratory using a method that is NGSP-certified and standardized to the DCCT assay), in the absence of unequivocal hyperglycemia, results should be confirmed by repeat testing
Prediabetes	FPG 5.6–7.0 mmol/L (5.6≤ FPG <7.0 mmol/L) [impaired fasting glucose (IFG)] or 2-h plasma glucose 7.8–11.1 mmol/L (7.8≤ 2h OGTT <11.1 mmol/L) following 75-g oral glucose load [impaired glucose tolerance (IGT)] or HbA1C range of 5.7-6.5% (5.7%≤ HbA1C <6.5%)
NGT	FPG 3.9–5.6 mmol/L (3.9≤ FPG <5.6 mmol/L) and 2-h plasma glucose ≤7.8 mmol/L following 75-g oral glucose load

T2DM, type 2 diabetes mellitus; NGT, normal glucose tolerance; HbA1c, glycosylated hemoglobin.

According to the criteria, there were 15 individuals with T2DM (7 men, 8 women; 51.0±8.0 years), 17 with prediabetes (3 men, 14 women; 54.0±6.7 years), and 16 with NGT (8 men, 8 women; 50.0±10.7 years). Exclusion criteria for all of the investigations were smoking, metallic implants, and medications (such as steroids or diet pills) that influence body adipose composition. Patients with chronic or acute viral hepatitis (hepatitis A, B, or C) and other forms of hepatic or pancreatic disease including drug-induced, autoimmune, chemically toxic, and alcoholic-induced forms were also excluded from this study. All of the diabetic patients included in this study were newly diagnosed without prior treatment.

All of the subjects underwent the following blood laboratory tests: glycosylated hemoglobin (HbA1c), fasting blood glucose (FBG), 30 minutes of blood glucose (30BG), 2-hour post-meal blood glucose (P2BG), cholesterol (CHOL), triglyceride (TG), high-density lipoprotein (HDL), low-density lipoprotein (LDL), alanine aminotransferase (ALT), aspartate aminotransferase (AST), long-acting insulin (Q insulin), homeostasis model assessment of insulin resistance (HOMA-IR), homeostasis model assessment β cell function (HOMA-β), insulin action index (IAI), and quantitative insulin sensitivity index (QIUCKI). All of the tests were measured using an AU5800 automatic biochemical analyzer (Beckman Coulter, Brea, CA, USA). Body mass index (BMI) was measured using the formula BMI = body weight (kg)/height^2 (m^2).

MRI examination

All of the enrolled subjects underwent MRI examinations using a 1.5-T MRI scanner (Brivo MR355, GE Healthcare, Chicago, IL, USA). Breathing training before MRI was performed to ensure optimal image quality. All of the patients underwent MRI scanning covering the diaphragm to the 4th lumbar vertebral body in a supine position. Three-plane localization imaging was obtained at the beginning of the examination. The IDEAL-IQ sequence was acquired with the following parameters: TR =15.6 ms, 6 echoes in each TR, TE1 =1.2–1.5 ms (increment: 1.23 ms, 6 echoes); flip angle, 8°; and slice thickness, 10 mm. The images were processed using the software provided by the manufacturer to create water-phase, fat-phase, in-phase, and out-phase images, along with R2* and fat fraction maps.

Measurement of VAT volume

Each participant's fat fraction maps were imported into the processing workstation (Vitrea fX VES, Vital, Minnetonka, MN, USA). The workstation distinguished different tissues according to their signal intensity and automatically selected adipose tissue. After auto-selection, a senior radiologist reviewed and removed the unqualified adipose tissue, such as subcutaneous adipose tissue. Adipose tissue was measured 3 times, and the mean value was identified as the final data. The VAT volume corresponding to the 2nd and 3rd lumbar vertebral levels (VATV L2 and VATV L3) were extracted, respectively, and the sum of VATV L2 and VATV L3 was then computed and considered the total VATV (*Figure 1*).

Measurement of hepatic and pancreatic PDFF

The MRI images were reviewed by a radiologist with more than 6 years of experience in abdominal imaging who was blinded to the clinical and biochemical data of all

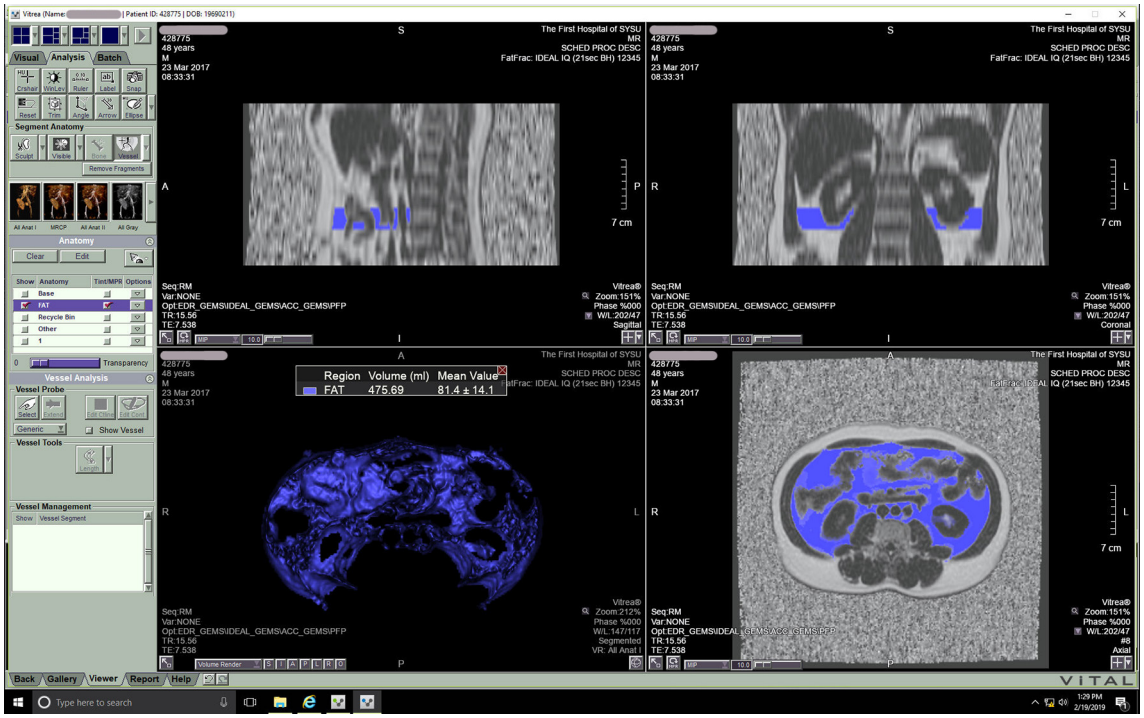

Figure 1 Illustration of adipose tissue measurement. Distribution of visceral adipose tissue at L3 level of a 48-year-old man with T2DM. T2DM, type 2 diabetes mellitus.

of the patients. The liver and pancreas PDFF levels were measured on the fat fraction maps using the workstation (AW 4.4, GE Healthcare). Hepatic PDFF levels were measured by placing 2 regions of interest (ROIs) each in the left and right lobes with an approximate ROI of 40–60 mm^2. One ROI each in the head, body, and tail of the pancreas of approximately 10–15 mm^2 was placed, and the PDFF of each ROI was measured. Then, the average liver and pancreas PDFF levels were calculated. All of the ROIs were surrounded by the tissue of interest to ensure that the ROIs were within the tissue of interest, avoiding major vessels, ducts, and collecting systems (*Figure 2*).

Statistical analysis

All statistical analyses were performed using SPSS (Version 20.0). The mean ± standard deviation described the continuous variables. The correlation analysis of VATV L2, VATV L3, and total VATV with each laboratory indicator was performed with the Spearman's rank correlation test. The differences in the continuous variables among the T2DM, prediabetes, and NGT groups were evaluated using one-way ANOVA or the Kruskal-Wallis H test according to the homogeneity of the variance test. The differences in the discrete variables among the T2DM, prediabetes, and NGT groups were evaluated using the chi-squared test. When there were statistical differences between all 3 groups, multiple comparisons were corrected using the Bonferroni method, and the corrected P value (P adjusted) was calculated by multiplying the P value with the number of tests performed (the number of tests in our study was 3). VATV L2, VATV L3, total VATV, and PDFF of the whole liver, whole pancreas, head, body, and tail of the pancreas were assessed for their ability to predict the presence of T2DM using the binary logistics regression model. A P value (or a P adjusted in the Bonferroni method) <0.05 was considered statistically significant.

Results

Correlation analysis of VATV L2, VATV L3, and total VATV with other clinical laboratory tests

HbA1c, 30BG, P2BG, TG, ALT, Q insulin, HOMA-IR, BMI, hepatic PDFF, and pancreatic PDFF showed a positive correlation (P<0.05) with VATV L2, VATV L3, and

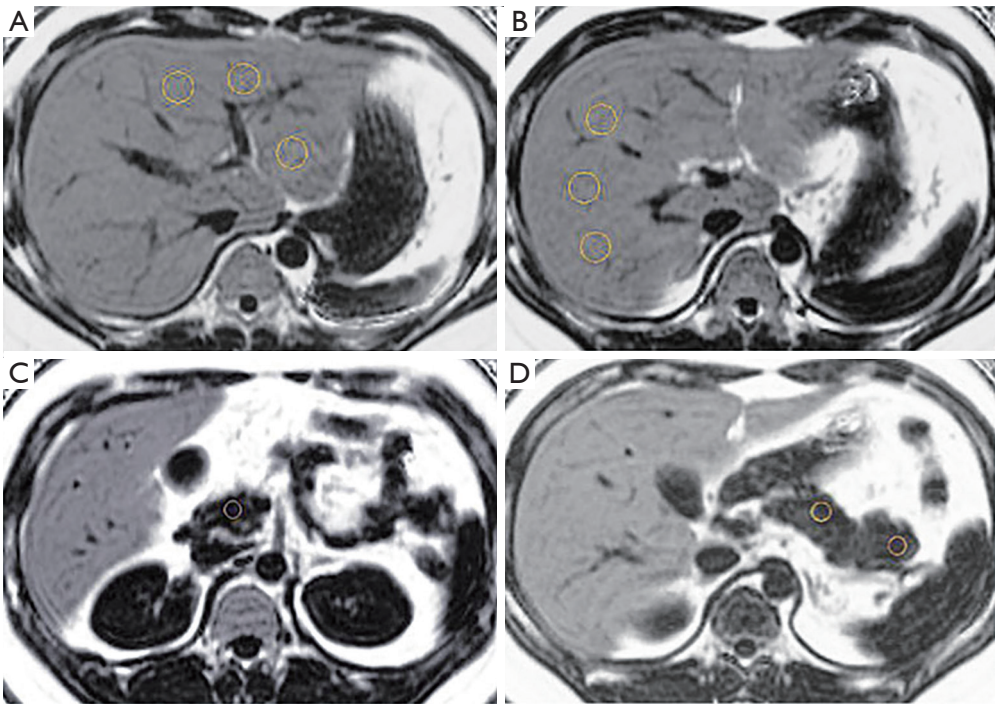

Figure 2 The ROIs (yellow circles) of the liver (A,B), pancreatic head (C), pancreatic body, and pancreatic tail (D). ROIs, regions of interest.

total VATV. HDL, IAI, and QUICKI showed a negative correlation (P<0.05) with VATV L2, VATV L3, and total VATV (*Table 2*).

The difference in visceral fat volume (VATV L2, VATV L3, and total VATV) in the T2DM, prediabetes, and NGT groups

The VATV L2, VATV L3, and total VATV values in the T2DM group were significantly higher than those in the prediabetes (VATV L2, P=0.03; VATV L3, P=0.006; and total VATV, P=0.008) and NGT groups (VATV L2, P=0.03; VATV L3, P=0.021; and total VATV, P=0.022. There was no statistically significant difference of the VATV L2, VATV L3, and total VATV values between the prediabetes and the NGT groups (VATV L2, P=1.00; VATV L3, P=1.00; and total VATV, P=1.00) (*Table 3*).

The difference in hepatic and pancreatic PDFF in the T2DM, prediabetes, and NGT groups

The hepatic PDFF in the T2DM group was significantly higher than that in the prediabetic (P=0.025, *Table 3*) and NGT groups (P<0.001), but there was no statistically significant difference in the hepatic PDFF between the prediabetes and NGT groups (P=0.58). The pancreatic PDFF in the T2DM group was significantly higher than that in the NGT group (whole pancreatic PDFF: P<0.001, pancreatic head PDFF: P=0.019, pancreatic body: P=0.001, and pancreatic tail PDFF: P<0.001). However, there was no statistically significant difference in the pancreatic PDFF between the T2DM and prediabetic groups (whole pancreatic PDFF: P=0.087, pancreatic head PDFF: P=0.189, pancreatic body: P=0.138, and pancreatic tail PDFF: P=0.159) or between the prediabetes and NGT groups (whole pancreatic PDFF: P=0.27, pancreatic head PDFF: P=1.00, pancreatic body: P=0.25, and pancreatic tail PDFF: P=0.10

Receiver operating characteristic (ROC) curve analysis

The visceral adipose volume (VATV L2, VATV L3, and total VATV), in combination with the hepatic PDFF and pancreatic PDFF, was used to predict the incidence of T2DM, prediabetes, and NGT, using ROC curve analysis. The area under the curve (AUC) of VATV L2 was 0.76 for predicting the presence of T2DM, which was statistically significant (P<0.01). The optimal threshold of VATV L2

Table 2 Correlation analysis of VATV L2, VATV L3, and total VATV with each laboratory indicator

Laboratory indicator	Correction coefficient and P value	VATV L2	VATV L3	Total VATV
PBF	Correlation coefficient	0.06	0.09	0.08
	P value	0.71	0.55	0.61
HbA1c	Correlation coefficient	0.49**	0.51**	0.52**
	P value	0.00	0.00	0.00
FBG	Correlation coefficient	0.25	0.26	0.27
	P value	0.08	0.08	0.06
30BG	Correlation coefficient	0.36*	0.32*	0.34*
	P value	0.01	0.03	0.02
P2BG	Correlation coefficient	0.45**	0.45**	0.46**
	P value	0.00	0.00	0.00
CHOL	Correlation coefficient	0.11	0.00	0.05
	P value	0.44	0.99	0.74
TG	Correlation coefficient	0.53**	0.51**	0.54**
	P value	0.00	0.00	0.00
HDL	Correlation coefficient	–0.58**	–0.69**	–0.65**
	P value	0.00	0.00	0.00
LDL	Correlation coefficient	0.13	0.08	0.11
	P value	0.37	0.57	0.47
ALT	Correlation coefficient	0.56**	0.45**	0.52**
	P value	0.00	0.00	0.00
AST	Correlation coefficient	0.27	0.11	0.19
	P value	0.06	0.46	0.20
Q insulin	Correlation coefficient	0.37*	0.32*	0.37*
	P value	0.01	0.03	0.01
HOMA -IR	Correlation coefficient	0.40**	0.35*	0.40**
	P value	0.00	0.01	0.00
HOMA-β	Correlation coefficient	0.15	0.06	0.10
	P value	0.32	0.68	0.48
IAI	Correlation coefficient	–0.40*	–0.35*	–0.40**
	P value	0.01	0.01	0.00
QUICKI	Correlation coefficient	–0.39*	–0.37*	–0.41**
	P value	0.01	0.01	0.00
BMI	Correlation coefficient	0.54**	0.57**	0.56**
	P value	0.00	0.00	0.00
Fat fraction of liver	Correlation coefficient	0.57**	0.54**	0.58**
	P value	0.00	0.00	0.00
Fat fraction of pancreas	Correlation coefficient	0.61**	0.68**	0.68**
	P value	0.00	0.00	0.00

*, P<0.05; **, P<0.01. VATV, visceral adipose tissue volume; FBG, fasting blood glucose; HDL, high-density lipoprotein; LDL, low-density lipoprotein; ALT, alanine aminotransferase; AST, aspartate aminotransferase; IAI, insulin action index; BMI, body mass index.

Table 3 The differences in the VATV L2, VATV L3, total VATV, PDFF of the whole liver, whole pancreas, head, body, and tail of the pancreas among the T2DM, prediabetes, and NGT groups

Variables	T2DM	Prediabetes	NGT	χ^2	P value	P value (P adjusted)		
						T2DM *vs.* prediabetes	T2DM *vs.* NGT	Prediabetes *vs.* NGT
VATV L2	569.15±241.61	398.04±89.97	387.66±187.39	8.43	0.01*	0.01 (0.03)*	0.01 (0.03)*	0.97 (1.00)
VATV L3	594.68±239.29	384.34±102.76	406.94±193.58	11.19	0.004**	0.002 (0.006)**	0.007 (0.021)*	0.72 (1.00)
Total VATV	1163.83±473.46	782.39±182.71	794.60±373.23	10.71	0.005**	0.003 (0.008)**	0.007 (0.022)*	0.76 (1.00)
Hepatic PDFF	12.22±4.45	9.54±6.01	7.20±2.96	15.41	<0.001***	0.008 (0.025)*	0.00 (0.00)***	0.19 (0.58)
Pancreatic PDFF	8.87±2.23	8.15±3.70	5.74±1.52	14.47	0.001**	0.029 (0.087)	0.00 (0.00)***	0.09 (0.27)
Pancreatic head PDFF	8.99±3.30	7.90±4.35	6.04±2.09	7.68	0.02*	0.063 (0.189)	0.006 (0.019)*	0.35 (1.00)
Pancreatic body PDFF	8.67±2.27	8.21±3.27	5.80±1.76	13.36	0.001**	0.046 (0.138)	0.00 (0.001)**	0.08 (0.25)
Pancreatic tail PDFF	8.67±2.37	8.35±3.83	5.40±1.43	15.68	<0.001***	0.053 (0.159)	0.00 (0.00)***	0.03 (0.10)

*, P<0.05; **, P<0.01; ***, P<0.001. P adjusted: multiple comparisons were corrected using the Bonferroni method. T2DM, type 2 diabetes mellitus; NGT, normal glucose tolerance; PDFF, proton-density fat fraction.

Figure 3 The receiver operating characteristic (ROC) curves of VAVT, hepatic PDFF, and pancreatic PDFF for predicting type 2 diabetes mellitus (T2DM). The area under ROC curve (AUC) for VAVT L2 was 0.76 (95% CI, 0.61–0.92, P<0.01), VATV L3 was 0.80 (95% CI, 0.66–0.94, P<0.01), total VATV was 0.80 (95% CI, 0.65–0.94, P<0.01), hepatic PDFF was 0.79 (95% CI, 0.65–0.92, P<0.01), and pancreatic PDFF was 0.75 (95% CI, 0.62–0.89, P<0.01).

to predict the diagnosis of T2DM was 460.34 mL, with a sensitivity of 73.33%, a specificity of 75.76%, and an accuracy of 75% (*Figure 3*).

The AUC of VATV L3 was 0.80 for predicting the diagnosis of T2DM with statistical significance (P<0.01). The optimal threshold of VATV L3 as a predictor of T2DM was 429.46 mL, with a sensitivity of 86.67%, a specificity of 72.73%, and an accuracy of 77.08%.

The AUC of the total VATV was 0.80 for predicting the diagnosis of T2DM with statistical significance (P<0.01). The optimal threshold of the total VATV as a predictor of T2DM was 887.83 mL, with a sensitivity of 86.67%, a specificity of 72.73%, and an accuracy of 77.08%.

The AUC of hepatic PDFF was 0.79 for predicting the presence of T2DM, which was statistically significant (P<0.01). The optimal threshold of hepatic PDFF to predict the diagnosis of T2DM was 6.75%, with a sensitivity of 100%, a specificity of 51.53%, and an accuracy of 66.67%.

The AUC of pancreatic PDFF was 0.75 for predicting the diagnosis of T2DM, which was with statistically significant (P<0.01). The optimal threshold of pancreatic PDFF as a predictor of T2DM was 6.02%, with a sensitivity of 100%, a specificity of 45.51%, and an accuracy of 62.54%.

The ROC curves of VATV L2, VATV L3, total VATV, hepatic PDFF, and pancreatic PDFF failed to predict the presence of prediabetes (VATV L2: P=0.16, VATV L3:

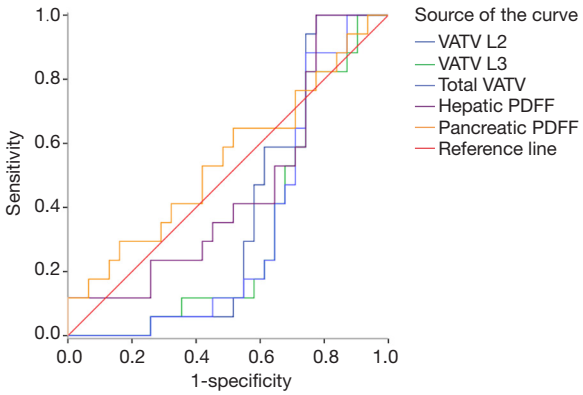

Figure 4 The receiver operating characteristic curves (ROC) of VAVT, hepatic PDFF, and pancreatic PDFF for predicting prediabetes. The area under ROC curve (AUC) for VAVT L2 was 0.38 (95% CI, 0.22–0.53, P=0.16), VATV L3 was 0.33 (95% CI, 0.17–0.48, P=0.05), total VATV was 0.33 (95% CI, 0.18–0.49, P=0.06), hepatic PDFF was 0.72 (95% CI, 0.65–0.92, P=0.64), and pancreatic PDFF was 0.75 (95% CI, 0.62–0.89, P=0.57).

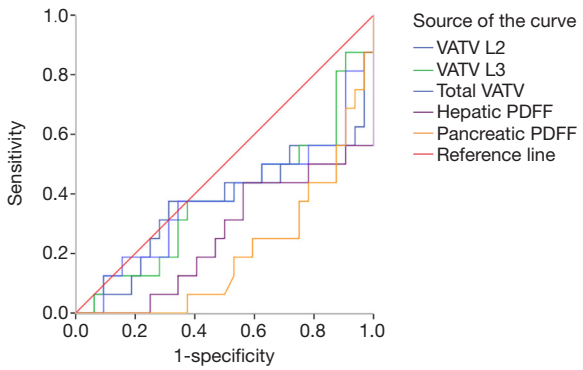

Figure 5 The receiver operating characteristic curves (ROC) of VAVT, hepatic PDFF, and pancreatic PDFF for predicting NGT. The area under ROC curve (AUC) for VAVT L2 was 0.37 (95% CI, 0.19–0.56, P=0.16), VATV L3 was 0.39 (95% CI, 0.21–0.56, P=0.20), and total VATV was 0.38 (95% CI, 0.20–0.57, P=0.20). NGT, normal glucose tolerance.

P=0.05, total VATV: P=0.06, hepatic PDFF, P=0.64; and pancreatic PDFF, P=0.57, *Figure 4*) and NGT (VATV L2: P=0.16, VATV L3: P=0.20, total VATV: P=0.20, hepatic PDFF, P=0.07; and pancreatic PDFF, P=0.16, *Figure 5*).

Binary logistics regression model analysis

Due to the lack of significant differences in the characteristics including gender, age, and BMI in the patients between the 3 groups, VATV L2, VATV L3, total VATV, and PDFF of the liver, pancreas, pancreatic head, body, and tail were used as independent variables to predict the presence of T2DM using binary logistics regression analysis. The results suggest that only VATV L3 demonstrated a statistically significant correlation with the presence of T2DM (P=0.01). An increase of 1 standard deviation in VATV L3 change was associated with a 1.01-fold increase in the odds of diabetes (OR, 1.01; 95% CI, 1.002–1.017). After adjusting the other variables, the predictive sensitivity, specificity, and accuracy of VATV L3 to predict the presence of T2DM were 80.00%, 88.20%, and 84.40%, respectively.

Discussion

Currently, ectopic adipose tissue deposit is recognized as one of the primary elements in the pathogenesis of IGT and T2DM (5-8). Given the focal accumulation of adipose tissue in the insulin-secreting organ with presumable effects on endocrine function, and excessive VAT disrupting multiple pathways in gluconeogenesis, significant interest has been focused on evaluating the fat content of the pancreas, liver, and VAT (17). Several studies have published reports on the correlation of T2DM with ectopic fat compartments, such as hepatic fat content, pancreatic fat content, and VAT (26-29). However, no previous studies have as yet investigated which of the 3 is more closely associated with T2DM. This study aimed to provide more insight into the independent association of ectopic fat deposition and T2DM.

The present cohort obtained from the general population demonstrated that there were significant differences in the visceral adipose volume in the T2DM, prediabetes, and NGT groups, with a continuous increase in VAT from NGT and prediabetes in patients with T2DM.

Also, compared with VATV L2, the results of the ROC analysis showed that the AUC value of VATV L3 was more consistent with that of the total VATV. Furthermore, VAVT L3 and total VATV demonstrated better correlations with the presence of T2DM than VATV L2, hepatic PDFF, and pancreatic PDFF. This suggests the better predictive value of VATV L3 with total VATV for predicting the presence of T2DM compared to VAVT L2, hepatic PDFF, and pancreatic PDFF. This finding is consistent with the conclusion of Schweitzer *et al.*, who proposed that the VAT accumulated on the 3rd lumbar vertebra level has a higher prediction effect for the whole-body VATV than any other level (23,24). This observation suggests the need

to consider the role of metabolic differences rather than the conventional understanding of quantitative differences in visceral adipose content for prediabetic and diabetic patients. Shen *et al.* pointed out a possible explanation which was intraperitoneal adipose tissue (IPAT) and extraperitoneal adipose tissue (EPAT) (30,31). Since EPAT depots serve primarily as the mechanical cushions of the organs, and IPAT components have substantial metabolic activities, greater IPAT of VAVT L3 may be why VATV L3 it demonstrates better correlations with total VATV even when the VAT readings may not be high.

Specifically, the result of binary logistics regression analysis suggests that, as opposed to VATV L2, total VATV, hepatic PDFF, and pancreatic PDFF, only VATV L3 was significantly associated with the presence of T2DM. Neeland *et al.* found that excessive visceral fat, rather than general adiposity, was independently associated with the incidence of T2DM (7,8). However, Yamazaki *et al.* reported that pancreatic fat content was positively associated with the incidence of T2DM, but a multivariate analysis showed that pancreatic fat content was not independently associated with future T2DM (13). Lack of an association between impaired beta cell function and pancreatic fat content was also reported in previous studies (12,14,32). All of the studies above indicate that the VAT can predict the occurrence of T2DM with better accuracy than the fat content of the liver and pancreas. VAT is a high-risk factor for the development of prediabetes and T2DM, which may be a result of its greater catecholamine-stimulated lipolysis and inflammation (33,34). Moreover, the 3rd lumbar vertebra level has a higher prediction effect for whole-body VATV than any other level (35). Therefore, VATV L3 is a better predictor of the presence of T2DM than VATV L2, total VATV, PDFF of the liver, or PDFF of the pancreas.

There are several limitations to this report. First, due to this study's strict inclusion criteria, every enrolled patient had to undergo a variety of examinations, resulting in a relatively small sample size. The small sample size may be accompanied by type II errors (23,24). Further studies with larger sample sizes are required to obtain more accurate findings. Second, this was a single-center study, so multi-center studies are required to explore the consistency in different ethnic populations. Finally, the term "abdominal VATV" in this study did not include pelvic visceral organs, so the results should be interpreted with caution.

In conclusion, the results indicate that VAVT was significantly higher in the subjects with T2DM compared to the prediabetic and healthy controls. The multivariable analysis indicated that VAVT L3 was the best predictor of T2DM compared to hepatic PDFF, pancreatic PDFF, VAVT L2, and total VATV. The measurement of abdominal adipose tissue at the optimal level will serve as an essential tool for the analysis of the effects of VATV on the presence of T2DM. Estimating VATV by noninvasive MRI may help identify individual predictive factors of potential metabolic diseases.

Acknowledgments

Funding: This study was supported by grants from the National Natural Science Foundation of China (No. 81801761, 81771908, 81571750, and 81770654).

Footnote

Conflicts of interest: The authors have no conflicts of interest to declare.

Ethical Statement: The study protocol was approved by the Institutional Review Board of Sun Yat-Sen University, and all of the patients enrolled provided written informed consent for participation. All of the procedures carried out in this study were in accordance with approved guidelines.

References

1. Emerging Risk Factors Collaboration, Sarwar N, Gao P, Seshasai SR, Gobin R, Kaptoge S, Di Angelantonio E, Ingelsson E, Lawlor DA, Selvin E, Stampfer M, Stehouwer CD, Lewington S, Pennells L, Thompson A, Sattar N, White IR, Ray KK, Danesh J. Diabetes mellitus, fasting blood glucose concentration, and risk of vascular disease: a collaborative meta-analysis of 102 prospective studies. Lancet 2010;375:2215-22.
2. Schneider AL, Kalyani RR, Golden S, Stearns SC, Wruck L, Yeh HC, Coresh J, Selvin E. Diabetes and Prediabetes and Risk of Hospitalization: The Atherosclerosis Risk in Communities (ARIC) Study. Diabetes Care 2016;39:772-9.
3. Dall TM, Yang W, Halder P, Pang B, Massoudi M, Wintfeld N, Semilla AP, Franz J, Hogan PF. The economic burden of elevated blood glucose levels in 2012: diagnosed and undiagnosed diabetes, gestational diabetes mellitus, and prediabetes. Diabetes Care 2014;37:3172-9.
4. James C, Bullard KM, Rolka DB, Geiss LS, Williams DE, Cowie CC, Albright A, Gregg EW. Implications of alternative definitions of prediabetes for prevalence in U.S.

adults. Diabetes Care 2011;34:387-91.
5. Bergman RN, Kim SP, Catalano KJ, Hsu IR, Chiu JD, Kabir M, Hucking K, Ader M. Why visceral fat is bad: mechanisms of the metabolic syndrome. Obesity (Silver Spring) 2006;14:16S-19S.
6. Middleton MS, Haufe W, Hooker J, Borga M, Dahlqvist Leinhard O, Romu T, Tunón P, Hamilton G, Wolfson T, Gamst A, Loomba R, Sirlin CB. Quantifying Abdominal Adipose Tissue and Thigh Muscle Volume and Hepatic Proton Density Fat Fraction: Repeatability and Accuracy of an MR Imaging-based, Semiautomated Analysis Method. Radiology 2017;283:438-49.
7. Neeland IJ, Turer AT, Ayers CR, Powell-Wiley TM, Vega GL, Farzaneh-Far R, Grundy SM, Khera A, McGuire DK, de Lemos JA. Dysfunctional adiposity and the risk of prediabetes and type 2 diabetes in obese adults. JAMA 2012;308:1150-9.
8. Wander PL, Boyko EJ, Leonetti DL, McNeely MJ, Kahn SE, Fujimoto WY. Change in visceral adiposity independently predicts a greater risk of developing type 2 diabetes over 10 years in Japanese Americans. Diabetes Care 2013;36:289-93.
9. Dong Z, Luo Y, Cai H, Zhang Z, Peng Z, Jiang M, Li Y, Li C, Li ZP, Feng ST. Noninvasive fat quantification of the liver and pancreas may provide potential biomarkers of impaired glucose tolerance and type 2 diabetes. Medicine 2016;95:e3858.
10. Macauley M, Percival K, Thelwall PE, Hollingsworth KG, Taylor R. Altered volume, morphology and composition of the pancreas in type 2 diabetes. PLoS One 2015;10:e0126825.
11. Heni M, Machann J, Staiger H, Schwenzer NF, Peter A, Schick F, Claussen CD, Stefan N, Häring HU, Fritsche A. Pancreatic fat is negatively associated with insulin secretion in individuals with impaired fasting glucose and/or impaired glucose tolerance: a nuclear magnetic resonance study. Diabetes Metab Res Rev 2010;26:200-5.
12. Kühn JP, Berthold F, Mayerle J, Völzke H, Reeder SB, Rathmann W, Lerch MM, Hosten N, Hegenscheid K, Meffert PJ. Pancreatic Steatosis Demonstrated at MR Imaging in the General Population: Clinical Relevance. Radiology 2015;276:129-36.
13. Yamazaki H, Tsuboya T, Katanuma A, Kodama Y, Tauchi S, Dohke M, Maguchi H. Lack of Independent Association Between Fatty Pancreas and Incidence of Type 2 Diabetes: 5-Year Japanese Cohort Study. Diabetes Care 2016;39:1677-83.
14. Begovatz P, Koliaki C, Weber K, Strassburger K, Nowotny B, Nowotny P, Müssig K, Bunke J, Pacini G, Szendrödi J, Roden M. Pancreatic adipose tissue infiltration, parenchymal steatosis and beta cell function in humans. Diabetologia 2015;58:1646-55.
15. Kim SY, Kim H, Cho JY, Lim S, Cha K, Lee KH, Kim YH, Kim JH, Yoon YS, Han HS, Kang HS. Quantitative assessment of pancreatic fat by using unenhanced CT: pathologic correlation and clinical implications. Radiology 2014;271:104-12.
16. Sepe PS, Ohri A, Sanaka S, Berzin TM, Sekhon S, Bennett G, Mehta G, Chuttani R, Kane R, Pleskow D, Sawhney MS. A prospective evaluation of fatty pancreas by using EUS. Gastrointest Endosc 2011;73:987-93.
17. Idilman IS, Tuzun A, Savas B, Elhan AH, Celik A, Idilman R, Karcaaltincaba M. Quantification of liver, pancreas, kidney, and vertebral body MRI-PDFF in non-alcoholic fatty liver disease. Abdom imaging 2015;40:1512-9.
18. Idilman IS, Aniktar H, Idilman R, Kabacam G, Savas B, Elhan A, Celik A, Bahar K, Karcaaltincaba M. Hepatic steatosis: quantification by proton density fat fraction with MR imaging versus liver biopsy. Radiology 2013;267:767-75.
19. Permutt Z, Le TA, Peterson MR, Seki E, Brenner DA, Sirlin C, Loomba R. Correlation between liver histology and novel magnetic resonance imaging in adult patients with non-alcoholic fatty liver disease - MRI accurately quantifies hepatic steatosis in NAFLD. Aliment Pharmacol Ther 2012;36:22-9.
20. Reeder SB, Cruite I, Hamilton G, Sirlin CB. Quantitative assessment of liver fat with magnetic resonance imaging and spectroscopy. J Magn Reson Imaging 2011;34:729-49.
21. Storz C, Heber SD, Rospleszcz S, Machann J, Sellner S, Nikolaou K, Lorbeer R, Gatidis S, Elser S, Peters A, Schlett CL, Bamberg F. The role of visceral and subcutaneous adipose tissue measurements and their ratio by magnetic resonance imaging in subjects with prediabetes, diabetes and healthy controls from a general population without cardiovascular disease. Br J Radiol 2018;91:20170808.
22. Demerath EW, Shen W, Lee M, Choh AC, Czerwinski SA, Siervogel RM, Towne B. Approximation of total visceral adipose tissue with a single magnetic resonance image. Am J Clin Nutr 2007;85:362-8.
23. Schweitzer L, Geisler C, Pourhassan M, Braun W, Glüer CC, Bosy-Westphal A, Müller MJ. Estimation of Skeletal Muscle Mass and Visceral Adipose Tissue Volume by a Single Magnetic Resonance Imaging Slice in Healthy Elderly Adults. J Nutr 2016;146:2143-8.

24. Schweitzer L, Geisler C, Pourhassan M, Braun W, Glüer CC, Bosy-Westphal A, Müller MJ. What is the best reference site for a single MRI slice to assess whole-body skeletal muscle and adipose tissue volumes in healthy adults? Am J Clin Nutr 2015;102:58-65.
25. American Diabetes Association. Executive summary: standards of medical care in diabetes—2013. Diabetes Care 2013;36:S4-10.
26. Barbarash O, Gruzdeva O, Uchasova E, Dyleva Y, Belik E, Akbasheva O, Karetnikova V, Kokov A. The role of adipose tissue and adipokines in the manifestation of type 2 diabetes in the long-term period following myocardial infarction. Diabetol Metab Syndr 2016;8:24.
27. Sambataro M, Perseghin G, Lattuada G, Beltramello G, Luzi L, Pacini G. Lipid accumulation in overweight type 2 diabetic subjects: relationships with insulin sensitivity and adipokines. Acta Diabetol 2013;50:301-7.
28. van Beek L, Lips MA, Visser A, Pijl H, Ioan-Facsinay A, Toes R, Berends FJ, Willems van Dijk K, Koning F, van Harmelen V. Increased systemic and adipose tissue inflammation differentiates obese women with T2DM from obese women with normal glucose tolerance. Metabolism 2014;63:492-501.
29. Neeland IJ, Hughes C, Ayers CR, Malloy CR, Jin ES. Effects of visceral adiposity on glycerol pathways in gluconeogenesis. Metabolism 2017;67:80-9.
30. Shen W, Punyanitya M, Wang Z, Gallagher D, St-Onge MP, Albu J, Heymsfield SB, Heshka S. Visceraladipose tissue: relations between single-slice areas and total volume. Am J Clin Nutr 2004;80:271-8.
31. Shen W, Chen J. Application of imaging and other noninvasive techniques in determining adipose tissue mass. Methods Mol Biol 2008;456:39-54.
32. van der Zijl NJ, Goossens GH, Moors CC, van Raalte DH, Muskiet MH, Pouwels PJ, Blaak EE, Diamant M. Ectopic fat storage in the pancreas, liver, and abdominal fat depots: impact on beta-cell function in individuals with impaired glucose metabolism. J Clin Endocrinol Metab 2011;96:459-67.
33. Liu A, McLaughlin T, Liu T, Sherman A, Yee G, Abbasi F, Lamendola C, Morton J, Cushman SW, Reaven GM, Tsao PS. Differential intra-abdominal adipose tissue profiling in obese, insulin-resistant women. Obes Surg 2009;19:1564-73.
34. Bolinder J, Kager L, Ostman J, Arner P. Differences at the receptor and postreceptor levels between human omental and subcutaneous adipose tissue in the action of insulin on lipolysis. Diabetes 1983;32:117-23.
35. So R, Matsuo T, Sasai H, Eto M, Tsujimoto T, Saotome K, Tanaka K. Best single-slice measurement site for estimating visceral adipose tissue volume after weight loss in obese, Japanese men. Nutr Metab (Lond) 2012;9:56.

Cite this article as: Wang M, Luo Y, Cai H, Xu L, Huang M, Li C, Dong Z, Li ZP, Feng ST. Prediction of type 2 diabetes mellitus using noninvasive MRI quantitation of visceral abdominal adiposity tissue volume. Quant Imaging Med Surg 2019;9(6):1076-1086. doi: 10.21037/qims.2019.06.01

